ASME Journal of Mechanisms and Robotics
Online journal at:
https://asmedigitalcollection.asme.org/mechanismsrobotics

Felix Trautwein[1]
Institute for Control Engineering of Machine Tools and Manufacturing Units (ISW), University of Stuttgart, Stuttgart 70174, Germany
e-mail: felix.trautwein@isw.uni-stuttgart.de

David Dietrich
Institute for Control Engineering of Machine Tools and Manufacturing Units (ISW), University of Stuttgart, Stuttgart 70174, Germany
e-mail: david.dietrich@isw.uni-stuttgart.de

Andreas Pott
Institute for Control Engineering of Machine Tools and Manufacturing Units (ISW), University of Stuttgart, Stuttgart 70174, Germany
e-mail: andreas.pott@isw.uni-stuttgart.de

Alexander Verl
Institute for Control Engineering of Machine Tools and Manufacturing Units (ISW), University of Stuttgart, Stuttgart 70174, Germany
e-mail: alexander.verl@isw.uni-stuttgart.de

Strategy for Topological Reconfiguration of Cable-Driven Parallel Robots

This paper presents a strategy for stable topological in-operation-reconfiguration of cable-driven parallel robots. The term topological refers to the addition or removal of active cables and thus to changing the topology of the cable robot. During the whole reconfiguration process, the strategy guarantees the stability of the platform by considering a stability criterion based on the potential energy. In this context, two new formulations of a stable and minimal-stable workspace are introduced. Consequently, the theoretical foundations of kinematics and statics are first presented. Based on this, the limitations of conventional modeling approaches in the context of topological reconfiguration are outlined and necessary adaptations of the modeling are made. Afterward, impacts of topological adaptations are analyzed, followed by a formal description and a strategy for topological in-operation-reconfiguration. Finally, the reconfiguration strategy is applied to two simulation experiments, which show that the method is suitable for determining a stable reconfiguration sequence for the desired adaptation of the robot. [DOI: 10.1115/1.4065642]

Keywords: cable-driven mechanisms, kinematics, dynamics, and control of mechanical systems, mechanism synthesis and analysis, mechanisms and robots, parallel mechanisms and robots, parallel robots

1 Introduction

Cable-driven parallel robots (CDPRs) are a special type of parallel robot where the moving platform is connected to the winches by parallel cables. Due to the cables as very light drive components, which can additionally be wound up on drums, CDPRs can have very large workspaces, as can be seen in *SkyCam* [1] or the field phenotyping platform [2] at the *Swiss Federal Institute of Technology* (ETH). Besides the robots mentioned above, there are several other CDPRs such as the *Cablerobot Simulator* [3] at *Max-Planck*, the *IPAnema*-family [4] at *Fraunhofer IPA*, or the *CoGiRo* [5] at *LIRMM*. Here, all the robots mentioned are redundantly restrained, but the system *CoGiRo* [5] is designed in a suspended configuration.

Due to the simplicity and modularity of cables as drive components and the ability to easily move the attachment points on the frame or platform, CDPRs offer a unique possibility of reconfiguration. Reconfiguration refers to the addition or removal of cables and displacement of attachment points. In particular, the additional term "topological" here refers to changing the number of active cables during operation and thus changing the topological structure of the CDPR. Exemplary demonstrator systems for reconfiguration experiments of CDPRs are *COPacabana* [6], *ReelAx* [7], *Segesta* [8], or the robot from Ref. [9]. The enterprise *Kuenz GmbH* offers the mobile gantry crane *Freerider RTG* [10], which uses eight separately controlled cables and is moved by a wheeled undercarriage, making it also a kind of reconfigurable CDPR.

Furthermore, studies on continuous reconfiguration of CDPRs are presented by Nguyen et al. [11–13]. The authors investigated a CDPR for large-scale aircraft maintenance and defined a method to determine an optimal configuration for a suspended CDPR considering continuous reconfigurable parameters. Other studies assuming continuous parameters are Trautwein et al. [14], Zhou et al. [15,16], and Reichert et al. [8]. Boumann and Bruckmann [17] employed a continuous reconfiguration option on the frame to stabilize the platform of a CDPR after cable failure.

Contrary to the aforementioned works, Gagliardini et al. [18,19] defined the reconfigurable parameters as part of a discrete set. Then, the discrete reconfiguration option is used to plan a collision-free path through a cluttered environment using graph representation and a discrete optimization method. Recently, Mishra et al. [20] used a discrete set of reconfigurable parameters to optimize the cable routing.

All these works share a common focus, which lies in the theoretical determination of the geometry of the CDPR according to a set of parameters and a given task or requirement. Consequently, the next step toward the practical validation or even the application of such a system is the transfer and implementation of the determined geometrical parameters at the practical CDPR. Usually, this means the appropriate placement of the anchor points on the frame and the platform. For CDPRs with continuously reconfigurable parameters, Reichert et al. [8] and Zhou et al. [15,16] used

[1]Corresponding author.

Contributed by the Mechanisms and Robotics Committee of ASME for publication in the Journal of Mechanisms and Robotics. Manuscript received November 10, 2023; final manuscript received April 25, 2024; published online June 17, 2024. Assoc. Editor: Stéphane Caro.

the implemented linear drives to continuously adjust the geometry according to the results of the planning process. For the adjustments for CDPRs with discrete parameters, Gagliardini [21] introduced the concepts of off-line reconfiguration and in-line reconfiguration. Here, the off-line reconfiguration is a static procedure, where the platform is placed on the ground and in-line reconfiguration addresses a scenario, where the platform remains in its pose and first all new cables are attached and tensioned, and second, the cables of the previous configuration are loosened and detached.

An example for practical use was done in the context of the EU project *CableBot,*[2] which demonstrated the semi-automatic handling and assembly of components. The cables are attached directly to the component and the component is moved to the desired position. When the desired position is reached, the cables are loosened and attached to the next part. Since the building parts are placed on the floor or attached to the another part, the handling scenario described corresponds to the concept of off-line reconfiguration. Thus, the strategies mentioned for achieving discrete reconfiguration are based either on the fact that there are more cables available than required for the CDPR (on-line) or that the platform can be placed on the floor (off-line).

So the mentioned strategies for the realization of a discrete reconfiguration rely either on the fact, that there are more cables available than required for the cable robot (on-line) or the platform can be placed on the floor (off-line). These two limitations lead us to the motivation and research question of the paper. How can a CDPR be reconfigured by adding or removing active cables in such a way that the platform remains stable in its pose, regardless of the number of active cables. This requires a suitable criterion for expressing the stability of the CDPR's platform for a varying number of cables. In this context, an approach for stability classification of CDPRs was presented by Behzadipour and Khajepour [22]. The authors defined the stiffness of a CDPR as the sum of the elastic stiffness and the stiffness caused by antagonistic forces [23]. The results are then transferred to a stability classification and thereupon a criterion for stabilizability for cable-driven mechanisms. Carricato and Merlet [24] introduced an approach to evaluate the stability of an under-constrained CDPR algebraically. First, an analytical solution for the static equilibrium of poses is derived and, based on this, the stability is defined by the positive definiteness of the Hessian matrix. Pott and Tempel [25] introduced an energy-based formulation of the forward kinematics for CDPRs. Since the algorithm is based solely on potential energy and does not require a specific number of cables or kinematic classification, it can be applied to CDPRs ranging from underconstrained to redundantly constrained systems, and in addition, different cable models can be integrated into the framework. Finally, the authors derived a stability measure based on the Hessian of the potential energy function of the CDPR and thus show the relationship between the geometric shape of the energy function and the stability of the CDPR.

In summary, the objective of our work is to develop a strategy for in-operation-reconfiguration for removing and adding active cables while ensuring that the platform remains within its defined stability limits. An existing definition for stability is applied to the problem and the novelty and contribution of the work lie in a general spatial modeling of the robots, a stable and minimal-stable workspace concept, and finally, the algorithm for the determination of the reconfiguration procedure.

In the structure of the paper, the necessary kinematic and static foundations are presented in Sec. 2. Section 3 formulates the deficits in existing modeling approaches and introduces the required extensions and adaptations. In Sec. 4, the strategy for topological reconfiguration is presented, followed by the simulative validations in Sec. 5. Finally, a conclusion and outlook are given in Sec. 6.

[2]https://www.youtube.com/watch?v=cu0XztEAQy4.

2 Theoretical Foundations

In the following, the kinematic fundamentals are first introduced, and based on this, the static definitions are derived. Both topics are required for the assessment of the platform stability during a topological reconfiguration procedure.

2.1 Kinematics. The starting point for the kinematic definitions is the loop closure from Fig. 1. It consists of the proximal anchor points A_i and the corresponding vectors $\boldsymbol{a}_i$, measured in the global coordinate frame $\mathcal{K}_0$. The distal anchor points B_i are described by $\boldsymbol{b}_i$ in terms of the platform coordinate frame $\mathcal{K}_P$. The position and orientation of the platform are expressed by the position vector $\boldsymbol{r}$ and the rotation matrix $\boldsymbol{R}$. Based on this, the pose vector is defined as $\boldsymbol{y} = (\boldsymbol{r}, \boldsymbol{R}) \in \mathbb{R}^n$, where n describes the number of degrees-of-freedom (DOF) of the platform (e.g., planar case: $n = 3$ and spatial case: $n = 6$). The ith cable vectors are normalized by their lengths l_i, resulting in the unit vectors $\boldsymbol{u}_i = \frac{\boldsymbol{l}_i}{|\boldsymbol{l}_i|}$ describing the direction of the cables. In this work, the cables are assumed to be massless, linear elastic, and straight, so the effect of sagging is neglected. In addition, the scalar cable lengths are collected in the vector $\boldsymbol{l} \in \mathbb{R}^m$, where m is the number of acting cables. Based on these kinematic definitions, the implicit and scalar loop closure is expressed as

$$\nu_i = \|\boldsymbol{a}_i - \boldsymbol{r} - \boldsymbol{R}\boldsymbol{b}_i - \boldsymbol{l}_i\|_2 = 0 \quad \text{for } i = 1, \ldots, m \tag{1}$$

According to Gosselin and Angeles [26], the collected loop closure equations $\boldsymbol{\nu}$ differentiated by the cable lengths and the pose yield to

$$\underbrace{\frac{\partial \boldsymbol{\nu}(\boldsymbol{y}, \boldsymbol{l})}{\partial \boldsymbol{y}}}_{\boldsymbol{J}_\mathrm{A}} \delta\boldsymbol{y} + \underbrace{\frac{\partial \boldsymbol{\nu}(\boldsymbol{y}, \boldsymbol{l})}{\partial \boldsymbol{l}}}_{\boldsymbol{J}_\mathrm{B}} \delta\boldsymbol{l} = \boldsymbol{0} \tag{2}$$

This leads us to the Jacobian $\boldsymbol{J}_\mathrm{A} \in \mathbb{R}^{m \times n}$ and $\boldsymbol{J}_\mathrm{B} \in \mathbb{R}^{m \times m}$. Based on the Jacobian matrices, three different types of singularities are distinguished as follows:

(1) $\boldsymbol{J}_\mathrm{A}$ is rank deficient: The pose is in a parallel singularity, which gains an additional DOF, called over-mobility.
(2) $\det(\boldsymbol{J}_\mathrm{B}) = 0$: The pose is in a serial singularity with a loss of DOF, referred to as under-mobility.
(3) $\det(\boldsymbol{J}_\mathrm{B}) = 0$ and $\boldsymbol{J}_\mathrm{A}$ is rank deficient: The pose is in an architectural singularity, generated by design parameters, which can be avoided by reasonable design, and is therefore not considered further.

It should be noted that when the term singular or singularity appears in the following parts of this paper, the definition of parallel singularity is meant. In the next section, the static foundations for classifying the stability of CDPRs are introduced.

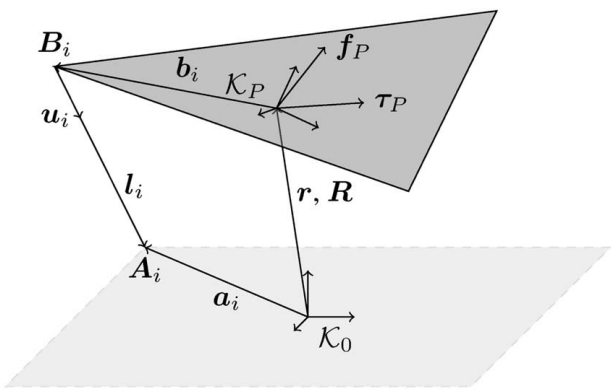

Fig. 1 Vector loop of a CDPR

2.2 Statics. For the static description, the external wrench $\boldsymbol{w}_\mathrm{P} \in \mathbb{R}^n$ acting on the platform is balanced by the collected cable forces $\boldsymbol{f} \in \mathbb{R}^m$

$$\boldsymbol{A}^\mathrm{T}(\boldsymbol{r}, \boldsymbol{R})\boldsymbol{f} + \boldsymbol{w}_\mathrm{P} = \boldsymbol{0} \quad \text{with}$$
$$\boldsymbol{A}^\mathrm{T}(\boldsymbol{r}, \boldsymbol{R}) = \begin{bmatrix} \boldsymbol{u}_1 & \cdots & \boldsymbol{u}_m \\ \boldsymbol{R}\boldsymbol{b}_1 \times \boldsymbol{u}_1 & \cdots & \boldsymbol{R}\boldsymbol{b}_m \times \boldsymbol{u}_m \end{bmatrix} \tag{3}$$

Here $\boldsymbol{A}^\mathrm{T} \in \mathbb{R}^{n\times m}$ denotes the pose-dependent structure matrix that distributes the cable forces on the degrees-of-freedom. The external wrench $\boldsymbol{w}_\mathrm{P}$ consists of the external forces $\boldsymbol{f}_\mathrm{P}$ and moments $\boldsymbol{\tau}_\mathrm{P}$. As a fundamental basis for assessing the stability during topological reconfiguration, the stiffness matrix (see Behzadipour and Khajepour [22]) is defined as the derivative of the structural equation in Eq. (3) as

$$\boldsymbol{K}_\mathrm{OS} = \frac{\partial \boldsymbol{w}_\mathrm{P}}{\partial \boldsymbol{y}} = \frac{\partial}{\partial \boldsymbol{y}}(-\boldsymbol{A}^\mathrm{T}\boldsymbol{f}) = \underbrace{-\boldsymbol{A}^\mathrm{T}\frac{\partial \boldsymbol{f}}{\partial \boldsymbol{y}}}_{\boldsymbol{K}_\mathrm{O}} \underbrace{-\frac{\partial \boldsymbol{A}^\mathrm{T}}{\partial \boldsymbol{y}}\boldsymbol{f}}_{\boldsymbol{K}_\mathrm{G}} \tag{4}$$

Hereby, the infinitesimally small variations describe the relations between changes in the pose and the acting external wrench. The resulting matrices are the operational stiffness matrix $\boldsymbol{K}_\mathrm{O} \in \mathbb{R}^{n\times n}$, which expresses the linear elasticity of the cables in terms of their stiffness coefficient k_i and the geometric stiffness matrix $\boldsymbol{K}_\mathrm{G} \in \mathbb{R}^{n\times n}$ that represents the effects of changes in the structure matrix. Based on this, Behzadipour and Khajepour [22] derived a stability and stabilizability criterion, which defines that a pose is stabilizable if the total stiffness matrix $\boldsymbol{K}_\mathrm{OS}$ can be made positive definite by a set of antagonistic cable forces under an arbitrary load. Antagonistic cable forces are usually generated by the redundant cable configuration, and increasing antagonistic forces lead to an increase in the total stiffness. In other words, the increasing antagonistic forces lead to an increasing energy E (see Sec. 3.4) and the pose can be stabilized for an arbitrary load. In summary, it can be stated, that the two necessary conditions for the stabilizability of a pose are that the pose is regular and there exists a cable force distribution to make the stiffness matrix positive definite, see Behzadipour and Khajepour [22]. The term regular means, that the pose is not singular for the examined CDPR. This fact is used in Sec. 3.4 for the definition of a stability criterion. So far, all the necessary kinematic and static foundations have been introduced and it is proceeded with the modeling of a topologically reconfigurable CDPRs.

3 Modeling of Topological Reconfigurable CDPRs

This section describes the impact of topological changes on the CDPR's model and the resulting problems, as well as outlining the need to extend the common modeling approaches. The formal description of the cable routing in terms of discrete sets is given and finally, the stability classification based on the extended model, the actual numerical criterion and its application to a (minimal-)stable workspace definition is presented. It should be noted, that the effects of pulleys and the drive train are neglected and the cables are assumed to be massless and linear elastic. In addition, interference between cables and between cables and objects are neglected.

3.1 Conventional Modeling and Resulting Deficits. In this paper, the identified deficits relate to the properties of the standard model of a CDPR, as it is usually used in the control system for motion planning. The standard model assumes that the cables are ideal straight lines and neglects effects from cables such as sagging. For a more detailed definition of the standard model, see Ref. [27].

Typically, the first step in designing a CDPR is to define a motion pattern and the number of cables required. The motion pattern defines the number of degrees-of-freedom and the translational or rotational direction in which they should act. An example motion pattern is a CDPR with a point-shaped platform that can move in three spatial directions. The most general motion pattern is a CDPR with an arbitrary platform that can move in six dimensions. Based on the chosen motion pattern and the application requirements, an appropriate geometry of the CDPR is determined. If the structure of the CDPR is to be reconfigured, at a later stage, the first option is to ensure that the motion pattern and number of active cables remain unchanged, thus maintaining the originally defined model. The second way is to allow the number of active cables to change, potentially violating basic modeling assumptions. This can lead to very practical problems, such as algorithms (e.g., inverse kinematics, cable force distribution, etc.) calculating incorrect results or even crashing due to numerical problems. The following list explains the two main deficits:

(1) Lack of formal description to express the changing cable configurations.
(2) Lack of a general modeling approach capable of handling changing numbers of degrees-of-freedom n and active number of cables m.

To overcome these deficits, the following sections introduce the formal description of a CDPR's configuration and the corresponding stability assessment of a configuration without requiring a constant number of n and m or a corresponding kinematic classification.

3.2 Discrete Configuration of a CDPR. Instead of the fixed definition of m anchor points on the frame and platform, all possible cable attachment points are grouped in two discrete sets as

$$\mathcal{A} = \{\boldsymbol{a}_1, \boldsymbol{a}_2, \ldots, \boldsymbol{a}_{j_a-1}, \boldsymbol{a}_{j_a}\} \quad \text{and}$$
$$\mathcal{B} = \{\boldsymbol{b}_1, \boldsymbol{b}_2, \ldots, \boldsymbol{b}_{j_a-1}, \boldsymbol{b}_{j_b}\} \tag{5}$$

Here $\mathcal{A}$ (number of elements j_a) represents the collection of all possible frame attachment points and $\mathcal{B}$ (number of elements j_b) represents the corresponding counterparts on the platform. In general, there are no restrictions on the number of elements j_a and j_b, and the method introduced later can handle both cases $j_a > j_b$ and $j_a < j_b$. The configuration is then defined by a set of two elements

$$c_i = \{c_{i,a}, c_{i,b}\} \tag{6}$$

from the two index sets

$$c_{i,a} \in \{1, 2, \ldots, j_a - 1, j_a\} \quad \text{and}$$
$$c_{i,b} \in \{1, 2, \ldots, j_b - 1, j_b\} \tag{7}$$

So the specific configuration c_i consists of two indices ($c_{i,a}$ and $c_{i,b}$) that run over the number of available indices in the sets of Eq. (5). Finally, a configuration of the CDPR with m cables is given as

$$\begin{aligned} \mathcal{C} &= \{\, c_1\,, \ldots,\, c_m\,\} \\ &= \{\{c_{1,a}, c_{1,b}\}, \ldots, \{c_{m,a}, c_{m,b}\}\} \end{aligned} \tag{8}$$

The configuration $\mathcal{C}$ is a nested set and is used to describe the cable routing. Notable configurations during the reconfiguration procedure are the set of the initial configuration $\mathcal{C}^\mathrm{init}$ with m^init cables and the final configuration $\mathcal{C}^\mathrm{fin}$ with m^fin cables.

3.3 Classification According to Solvability. Classifications of CDPRs are, e.g., the distinction into spatial or planar systems and additionally the classification according to the degree of redundancy $r = m - n$ introduced by Ming and Higuchi [28,29]. They introduced three different cases: incompletely-restrained-positioning-mechanism (IRPM), completely-restrained-positioning-mechanism (CRPM), and redundantly-restrained-positioning-mechanism (RRPM). From a design and development point of view, this is a simple and reasonable approach to significantly reduce the solution space of the design task. However, it is not

suitable for assessing the stability of the robot during topological changes. The reason for this is that changing the active cables goes hand in hand with changing the classification, which leads to theoretically deficient robot states such as singular poses, although this may be exactly what is intended. A practical example of such a system is presented by Kraus et al. [30]. The authors examined a planar CDPR, which is part of the RRPM class when modeled as a planar system with three DOF. However, when the system is embedded in the spatial domain with six DOF, the stiffness perpendicular to the robot's plane theoretically vanishes and is thus a singularity, and the robot changes its classification to IRPM. If we transfer this observation to our topological reconfiguration problem, we can state that we should avoid using a kinematic classification, and, as a consequence of that, avoid using classification-specific algorithms or analysis methods to describe the CDPR. The challenge that arises is that the CDPR must be modeled for the most general case, the spatial domain with six DOF, regardless of the actual configuration. Otherwise, the transition between kinematic classifications will lead to situations where model assumptions or the model itself become invalid, leading to problems like numerical problems or crashing algorithms. Measures to avoid the mentioned problems are described later in this section. In order to define a measure to express the state of the robot, the criterion of *Solvability* is introduced. Thus, the pose-dependent structure matrix $\boldsymbol{A}^{\mathrm{T}}(\boldsymbol{y})$ and the external wrench vector $\boldsymbol{w}_{\mathrm{P}}$ are assembled columnwise as

$$\boldsymbol{A}^{\mathrm{T}^*}(\boldsymbol{y}) = [\boldsymbol{A}^{\mathrm{T}}(\boldsymbol{y}) | \boldsymbol{w}_{\mathrm{P}}] \tag{9}$$

Here $\boldsymbol{A}^{\mathrm{T}^*}(\boldsymbol{y})$ is called the extended structure matrix. If the rank of the extended structure matrix satisfies the equation

$$\mathrm{rank}\boldsymbol{A}^{\mathrm{T}^*}(\boldsymbol{y}) = \mathrm{rank}\boldsymbol{A}^{\mathrm{T}}(\boldsymbol{y}) \tag{10}$$

the external wrench depends linearly on the operating directions of the cables. The structural equation from Eq. (3) is therefore solvable, but the feasibility of the resulting forces must be checked. Otherwise, if $\mathrm{rank}\boldsymbol{A}^{\mathrm{T}^*}(\boldsymbol{y}) > \mathrm{rank}\boldsymbol{A}^{\mathrm{T}}(\boldsymbol{y})$, the cables cannot support the external wrench in the given pose. To solve cable force calculations for CRPM or RRPM, one possible approach is to use the closed-form calculation of Pott et al. [31]. In this approach, the pseudoinverse of the structure matrix is calculated as

$$\boldsymbol{A}^{+\mathrm{T}} = \boldsymbol{A}(\boldsymbol{A}^{\mathrm{T}}\boldsymbol{A})^{-1} \tag{11}$$

For singular robots or singular poses, the aforementioned computational approach cannot be applied, because the Moore–Penrose pseudoinverse (MPP) does not exist. With reference to the exemplary scenario for the spatially studied planar system from Sec. 3.3, the closed-form solution for the MPP can not be calculated, although there exists a feasible solution. This is due to the fact that the system is modeled with six DOF and is thus strong rank deficit. The described system becomes solvable when the structure equation is transformed so that the redundant zero columns from $\boldsymbol{A}^{\mathrm{T}}$ can be identified and removed from the system of equations. The MPP is then invertible again, and the equation can be solved in the same way as known for redundant restraint CDPRs. If the MPP is not invertible, the inversion from Eq. (11) is not valid and the cable force calculation from Pott et al. [31] fails. This transformation of the structure matrix can be done, e.g., by applying Gaussian elimination, alternatively, singular value decomposition. This corresponds to a regression of the cable forces which neglects singular directions if Eq. (10) is satisfied. Finally, the criteria to be taken to model the CDPR so that the topological adaptations can be described are presented in the following list:

(1) Description of the CDPR in spatial domain with six DOF.
(2) Evaluation of the solvability criterion.
(3) If the criterion is fulfilled either transform the system to a low-dimensional subsystem or proceed directly.
(4) Calculation of the cable force distribution.
(5) Apply stabilizability criterion from Behzadiour and Khajepour [22].

The following section describes how the criterion of solvability and stabilizability is applied to a definition of stability in topological reconfiguration.

3.4 Energy-Based Stability Condition. As shown by Behzadipour and Khajepour [22], stability can be expressed by the virtual work done on the end effector when it undergoes an infinitesimally small displacement. According to this, the virtual work on the end effector is

$$E = \delta\boldsymbol{y}^{\mathrm{T}}\delta\boldsymbol{w}_{\mathrm{P}} = \delta\boldsymbol{y}^{\mathrm{T}}\boldsymbol{K}_{\mathrm{OS}}\delta\boldsymbol{y} \quad \text{and} \quad \boldsymbol{\lambda} = \boldsymbol{v}^{\mathrm{T}}\boldsymbol{K}_{\mathrm{OS}}\boldsymbol{v} \tag{12}$$

For an arbitrary small displacement $\delta\boldsymbol{y}$ and its induced forces $\delta\boldsymbol{w}_{\mathrm{P}}$, only the influence of its stiffness $\boldsymbol{K}_{\mathrm{OS}}$, is considered, which leads to an eigenvalue problem with normalized eigenvectors $\boldsymbol{v}_i$, collected in the matrix $\boldsymbol{v} \in \mathbb{R}^{n\times n}$. The corresponding eigenvalues λ_i are then collected in the matrix of eigenvalues $\boldsymbol{\lambda} \in \mathbb{R}^{n\times n}$. Considering the eigenvalues from Eq. (12), the following stability classification is made:

(1) Stable pose:

$$\hat{\boldsymbol{y}} = \{\boldsymbol{y} \in SE_3 \mid \lambda_i > 0 \ \forall \ i = 1 \ldots n\} \tag{13}$$

(2) Labile pose:

$$\bar{\boldsymbol{y}} = \{\boldsymbol{y} \in SE_3 \mid \exists\lambda_i = 0 \wedge \nexists\lambda_i < 0\} \tag{14}$$

(3) Unstable pose:

$$\check{\boldsymbol{y}} = \{\boldsymbol{y} \in SE_3 \mid \exists\lambda_i < 0\} \tag{15}$$

Finally, it should be mentioned, that the introduced stability assessment of a pose is based on linearization and is therefore only valid in a small neighborhood around the examined pose. In the next section, an overall criterion based on the introduced solvability and energy-based pose stability is given and applied to a corresponding workspace definition.

3.5 Stability Criterion and Stable Workspace Definition. The stability of a pose for topological reconfiguration consists of three different factors. First, the rank condition from Sec. 3.3, second, the signs of the eigenvalues of the stiffness matrix from Sec. 3.4, and third, the condition for the cable forces $f_i > 0$. Using this, the stable workspace is defined as the union of all poses, that satisfy the criteria as

$$\begin{aligned}\mathcal{W}_{\mathrm{s}}(\boldsymbol{w}_{\mathrm{P}}) = \{\boldsymbol{y} \in SE3 \mid \mathrm{rank}\boldsymbol{A}^{\mathrm{T}} = \mathrm{rank}\boldsymbol{A}^{\mathrm{T}^*} \wedge \\ \lambda_i > 0 \ \forall \ i = 1 \ldots n \wedge \ f_i > 0\}\end{aligned} \tag{16}$$

By weakening the eigenvalue criterion the minimal-stable workspace is defined as

$$\begin{aligned}\mathcal{W}_{\mathrm{ms}}(\boldsymbol{w}_{\mathrm{P}}) = \{\boldsymbol{y} \in SE3 \mid \mathrm{rank}\boldsymbol{A}^{\mathrm{T}} = \mathrm{rank}\boldsymbol{A}^{\mathrm{T}^*} \wedge \\ \lambda_i \geq 0 \ \forall \ i = 1 \ldots n \wedge \ f_i > 0\}\end{aligned} \tag{17}$$

Since, both the stable workspace $\mathcal{W}_{\mathrm{s}}$ and the minimal-stable workspace $\mathcal{W}_{\mathrm{ms}}$ can be evaluated pointwise, we apply the line-search and triangulation approach of Pott et al. [32] to capture the spatial domain enclosed by the hull of the workspace. It should be noted that the authors are aware of the limitations of the approach and that there may be poses within the hull that violate the stability criterion, but usually we are dealing with well-designed robots and additionally, the approach seems to be reasonable to plan the reconfiguration sequence. The term "well-designed" means that we do not consider CDPRs that have, e.g., a very obscure or asymmetric configuration or holes in the workspace. So the focus is on robots that have already been built and can be used in a real application. So far in this section, we have introduced the criteria for assessing the stability of a pose and finally formulated a definition to express

the stable workspace. Based on this, the following section presents a formal description of the reconfiguration process and introduces a two-step approach to determine a stable set of topological reconfigurations.

4 Strategy for Topological Reconfiguration

This chapter presents the strategy for determining the topological reconfiguration sequence. It formalizes the procedure, divides it into two sub-problems, and finally presents the algorithm for solving the reconfiguration problem.

4.1 Formal Description of Topological Reconfiguration.

For topological reconfiguration, a procedure is sought that allows attaching and detaching the needed cables in a practical order so that the platform stays stable in a single pose. The problem is described as

$$\begin{aligned} \mathcal{C}^{\text{init}} &= \{\{c_1^{\text{init}}\}, \ldots, \{c_m^{\text{init}}\}\} \rightarrow \\ \mathcal{C}^{\text{fin}} &= \{\{c_1^{\text{fin}}\}, \ldots, \{c_m^{\text{fin}}\}\} \end{aligned} \tag{18}$$

For the case

$$\{\mathcal{W}^{\mathcal{C}^{\text{init}}} \cap \mathcal{W}^{\mathcal{C}^{\text{fin}}}\} = \varnothing \tag{19}$$

that the workspaces of the initial configuration $\mathcal{W}^{\mathcal{C}^{\text{init}}}$ and the final configuration $\mathcal{W}^{\mathcal{C}^{\text{fin}}}$ do not overlap the intersection of the sets is empty, which is denoted by an empty set $\varnothing$. The indices for the stable and minimal-stable workspaces are omitted here for clarity. If there is no additional index as a subscript, the symbol refers to the stable or the minimal-stable workspace. The intersection of two sets is denoted by the operator $\cap$. Thus, so-called transition configurations are inserted as

$$\mathcal{C}^{\text{init}}(\boldsymbol{y}_1) \rightarrow \mathcal{C}^{\text{tra}}(\boldsymbol{y}_1) \quad \text{and} \quad \mathcal{C}^{\text{tra}}(\boldsymbol{y}_2) \rightarrow \mathcal{C}^{\text{fin}}(\boldsymbol{y}_2) \tag{20}$$

This splits the process from initial to final configuration and introduces a transition configuration $\mathcal{C}^{\text{tra}}$, whose workspace $\mathcal{W}^{\mathcal{C}^{\text{tra}}}$ bridges the gap between initial and final configuration. Changing configurations $\mathcal{C}^{\text{init}} \rightarrow \mathcal{C}^{\text{tra}}$ and $\mathcal{C}^{\text{tra}} \rightarrow \mathcal{C}^{\text{fin}}$ are done at the poses $\boldsymbol{y}_1$ and $\boldsymbol{y}_2$, respectively. Here the conditions for the reconfiguration poses are

$$\boldsymbol{y}_1 \in \mathcal{W}^{\mathcal{C}^{\text{init}}} \cap \mathcal{W}^{\mathcal{C}^{\text{tra}}} \quad \text{and} \quad \boldsymbol{y}_2 \in \mathcal{W}^{\mathcal{C}^{\text{tra}}} \cap \mathcal{W}^{\mathcal{C}^{\text{fin}}} \tag{21}$$

In order to minimize the necessary cable adaptations, the transition configuration

$$\mathcal{C}^{\text{tra}} = \{\{c_1^{\text{tra}}\}, \ldots, \{c_m^{\text{tra}}\}\} \in \{\mathcal{C}^{\text{init}} \cup \mathcal{C}^{\text{fin}}\} \tag{22}$$

is composed, if possible, by the paired elements of attachment points of the initial and final configurations. Here $m^{\text{tra}} \leq m_{\max}$ holds, which means that the number of active cables m^{tra} must be lower or equal to the number available cables $m_{\max}$. If the condition Eq. (19) is true again, a recursive subdivision by multiple transition configurations is performed until the workspaces of the initial and final configurations are connected by the workspaces of the transition configurations. In contrast to the transition configurations above, the configuration change at a given pose is formally described as

$$\mathcal{C}^0(\boldsymbol{y}) \rightarrow \mathcal{C}^k(\boldsymbol{y}) = \{\mathcal{C}^0, \mathcal{C}^1, \ldots, \mathcal{C}^{k-1}, \mathcal{C}^k\}(\boldsymbol{y}) \tag{23}$$

In this way, the actual configuration change is broken down into a sequence of elementary operations that represent either the addition or removal of a cable. The difference between two successive sets is always

$$|\mathcal{C}^{i-1} \triangle \mathcal{C}^i| = 1 \tag{24}$$

The operator $|\cdot|$ describes the number of elements in each set and the operator $\mathcal{A}\triangle\mathcal{B}$ evaluates the symmetric difference of two sets, here denoted by $\mathcal{A}$ and $\mathcal{B}$. The symmetric difference of two sets determines the elements that are in one of the sets but not in both. So the symmetric difference $\mathcal{A}\triangle\mathcal{B}$ is used instead of the common set difference $\mathcal{A} \setminus \mathcal{B}$, since both cases of adding and removing of cables have to be considered. Obviously, the condition $m^i \leq m_{\max}$ also holds. The pose

$$\boldsymbol{y} \in \bigcap_{i=0}^{k} \mathcal{W}_{\text{ms}}^{\mathcal{C}^i} \tag{25}$$

must be a non-labile or labile pose of every occurring minimal-stable workspace $\mathcal{W}_{\text{ms}}^{\mathcal{C}^i}$ (see Eq. (17)) of the corresponding intermediate configuration $\mathcal{C}^i$. The workspaces $\mathcal{W}_{\text{ms}}^{\mathcal{C}^i}$ are determined for a constant load on the platform $\boldsymbol{w}_{\text{P}}$, which is assumed to be just the gravitational force of the platform mass m_{P}. If the workspaces of the initial and final configurations don't overlap and the condition from Eq. (25) is false, a transition configuration must be introduced. Based on this introduced two-step approach consisting of a transition and intermediate configurations, the following section presents an algorithm to determine them in a way that ensures the stability of the platform.

4.2 Determination of the Topological Reconfiguration Procedure.

This section introduces a heuristic method for determining the transition configuration $\mathcal{C}^{\text{tra}}$ and an algorithm that identifies the necessary intermediate configurations $\mathcal{C}^k$ for a given platform pose.

4.2.1 Transition Configuration. For the transition configuration heuristic, it is assumed that the missing workspace intersection in Eq. (19) is due to the required feasibility of cable forces and not due to cable length limitations or collisions between cables or between cables and objects. This can occur if the enveloping polyhedrons of the attachment points at the base $\boldsymbol{a}_i$ of both configurations do not overlap. To reduce the number of necessary transition configurations, the configurations with the largest base area are considered first and all available cables j_a are included in the calculation procedure. To express both facts, the theoretical distance

$$\begin{aligned} d_i &= \left| \boldsymbol{a}_{c_{i,a}} - \frac{\sum_i^{j_a} \boldsymbol{a}_{c_{i,a}}}{|\mathcal{C}^{\text{init}} \cup \mathcal{C}^{\text{fin}}|} \right| \text{ with} \\ c_{i,a} &\in \{\mathcal{C}^{\text{init}} \cup \mathcal{C}^{\text{fin}}\} \end{aligned} \tag{26}$$

is introduced. The equation determines the distance d_i for each kinematic loop in terms of the anchor points $\boldsymbol{a}_{c_{i,a}}$ that are part of the union of the initial and final configurations $\{\mathcal{C}^{\text{init}} \cup \mathcal{C}^{\text{fin}}\}$, subtracted by the mean of all anchor points of the unified set. Thus, this corresponds to a virtual midpoint of all possible configurations. Then the cable connections with the greatest distance d_i are selected in descending order until the maximum number of cables $m_{\max}$ is reached. If the selection of cables is still not clear at the end, further properties of the cables of the initial and final configurations can be taken into account or the selection can be made randomly. One possible criterion is that an anchor point on the frame should appear only once in the transitions configuration, thus excluding situations where two cables share a common anchor point, which is a practical restriction to avoid such situations.

4.2.2 Intermediate Configuration. The stable pose of an intermediate reconfiguration lies in the intersection of the minimum-stable workspaces of all intermediate configurations on the way from an initial configuration to a required transition configuration

or to the respective final configuration. In general, the determination of intermediate configurations depends only on the available cables and the stability criterion mentioned above. There are therefore a total of $|\mathcal{C}^0 \triangle \mathcal{C}^k|!$ different combinations of how to get from the starting to the desired configuration. Note that there are no intermediate configurations to consider for the following situations:

(1) For the case $|\mathcal{C}^0 \setminus \mathcal{C}^k| = 0 \ \vee \ |\mathcal{C}^k \setminus \mathcal{C}^0| = 0$ no further intermediate configurations need to be considered. Hereby, the first term $|\mathcal{C}^0 \setminus \mathcal{C}^k| = 0$ expresses that there is no element that is part of $\mathcal{C}^0$ and $\mathcal{C}^k$ and therefore only cables need to be added. Similarly, the second term $|\mathcal{C}^k \setminus \mathcal{C}^0| = 0$ describes the opposite situation, where only cables need to be removed. In both situations, it is assumed that the initial and final configurations are both (minimal)-stable. If only cables are to be removed, all cables are slackened and removed in one step. If only cables are to be added, all cables are installed in one step and then tensioned together in the final and (minimal)-stable configuration. Assuming that the cables are massless, the reconfiguration is not expected to affect the stability of the platform. In both cases, it is not necessary to consider the intermediate configurations with their associated workspaces.
(2) There exists a maximum configuration, such that, the following condition is true $|\mathcal{C}^0 \cup \mathcal{C}^k| \leq m_{\max}$. In this case, all the required cables can be added first, followed by the removal of the obsolete cables. This case corresponds to the procedure introduced by Gagliardini [21].
(3) As the last case, there exists a stable or minimal-stable pose $\boldsymbol{y} \in \mathcal{W}^{\{\mathcal{C}^0 \cap \mathcal{C}^k\}} = \varnothing$. Thus, the obsolete cables are removed first, until the minimal configuration is reached.

If none of the above is the case, the sequence of intermediate configurations must be determined using an algorithm that ensures platform stability. This procedure is presented in the following section.

4.2.3 Algorithm for Determination of the Intermediate Configurations. The procedure is defined as a recursive method, starting at $\mathcal{C}^0$ and applying the elementary topological reconfiguration options until either $\mathcal{C}^k$ is reached or every possibility has been explored and there is no solution to the procedure. For better understanding, the search scheme for finding a suitable path from $\mathcal{C}^0$ to $\mathcal{C}^k$ via certain intermediate configurations is shown in Fig. 2. Here, the tree structure extends in two directions, the vertical depth and the horizontal width of the tree. As can be seen in Fig. 2, the vertical depth is indexed using i as superscript and the horizontal width is indexed using q as subscript.

The algorithm starts on the left side at $\mathcal{C}_1^1$ and determines all possible permutations that can be realized by an elementary reconfiguration operation. It then begins to iterate through the permutations, checking for feasibility. In the branch from $\mathcal{C}_1^1$ it can be seen that the configuration $\mathcal{C}_1^2$ turns out to be infeasible and so the algorithm proceeds to $\mathcal{C}_2^2$, while the algorithm detects an infeasible configuration one iteration depth deeper at $\mathcal{C}_1^3$ and consequently returns to the top level. This procedure corresponds to the "Depth-first search" from the field of graph search techniques. The successful completion of the search is demonstrated on the right branch, where there is a feasible transition from $\mathcal{C}^0 \rightarrow \mathcal{C}_q^1 \rightarrow [\ldots] \rightarrow \mathcal{C}_4^i \rightarrow \mathcal{C}^k$. The respective general algorithm for an arbitrary sequence is illustrated in Fig. 3 by means of a flowchart and additionally, the following list shows the step-by-step procedure:

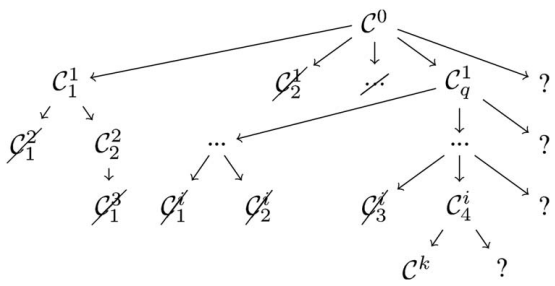

Fig. 2 Search tree for configurations

(1) The input values for the algorithm are the desired reconfiguration pose $\boldsymbol{y}$, the initial configuration $\mathcal{C}^0$, and the target configuration $\mathcal{C}^k$.
(2) Check whether the actual and target configurations match and, if so, return the initial configuration as result.
(3) Determine all possible permutations of the given configuration, which can be achieved by adding $\mathcal{C}^k \setminus \mathcal{C}^0$ or removing $\mathcal{C}^0 \setminus \mathcal{C}^k$ a cable, as long as the condition $m \leq m_{\max}$ is true.
(4) Check whether the given pose $\boldsymbol{y}$ satisfies the stable workspace criterion.
(5) For each feasible configuration, repeat steps (2)–(5) recursively.
(6) If step (5) returns a feasible configuration sequence, the sought sequence has been successfully determined and the algorithm terminates.
(7) If no sequence can be found, the algorithm returns an empty list and there is no stable reconfiguration sequence for the given inputs.

The result of the algorithm is successful, if it returns a sequence of topological reconfigurations. This work focuses on the determination of any possible solution, disregarding optimality criteria such as calculation time or minimization of cable adoptions. Such improvements are the subject of future work.

5 Simulation Experiments

The presented method for topological reconfiguration planning is demonstrated on a model which is mainly inspired by the *COPacabana* [6] at ISW. The assumed platform mass is $m_{\mathrm{P}} = 20\,\mathrm{kg}$ and the cable force limits are defined as $f_{\min} = 5\,\mathrm{N}$ and $f_{\min} = 1600\,\mathrm{N}$. The stiffness coefficient for the cables is defined as $k_i = 90\,\mathrm{GPa}$, a common value for 6 mm *Dyneema*© cables. It is assumed that the anchor points on the frame are mounted on a cuboid frame with edge lengths of $l_{\mathrm{F}} = 5.4\,\mathrm{m}$, width $w_{\mathrm{F}} = 4\,\mathrm{m}$, and height $h_{\mathrm{F}} = 3.66\,\mathrm{m}$. There are also attachment points halfway between the corners of the cuboid, giving a total of 20 regularly distributed anchor points on the frame. For the platform it is assumed that there are no additional anchor points and that the cables are attached to the corners of a cuboid with the dimensions $l_{\mathrm{P}} = 0.8\,\mathrm{m}$, $w_{\mathrm{P}} = 0.7\,\mathrm{m}$, and $h_{\mathrm{P}} = 0.3\,\mathrm{m}$. This results in eight possible anchor points on the platform. The anchor points on the platform are numbered 1–4 on the upper level and 5–8 on the lower level. As shown in Fig. 4, the global coordinate frame is placed in the bottom left corner of the frame and the axes are aligned according to the edges of the cuboid. The index of the potential anchor points starts at the coordinate origin with $c_{i,a} = 1$ and is incremented clockwise on the lower plane until $c_{i,a} = 8$. The index runs from the top left corner as $c_{i,a} = 9, \ldots, 16$. The remaining indices on the mid plane run over $c_{i,a} = 17, \ldots, 20$. The starting point for the reconfiguration planning is also shown in Fig. 4. At the beginning, the robot is installed in the left part of the frame and a changed task requires that the installation space on the right side is covered, so it is necessary to reconfigure the robot during operation so it can operate there. Thus, the initial configuration $\mathcal{C}^{\mathrm{init}}$ and the final configuration $\mathcal{C}^{\mathrm{fin}}$ are defined as

$$\begin{aligned} \mathcal{C}^{\mathrm{init}} &= \{\{1,1\},\{3,2\},\{4,3\},\{8,4\}, \\ &\quad \{9,5\},\{11,6\},\{12,7\},\{16,8\}\} \quad \text{and} \\ \mathcal{C}^{\mathrm{fin}} &= \{\{8,1\},\{4,2\},\{5,3\},\{7,4\}, \\ &\quad \{16,5\},\{12,6\},\{13,7\},\{15,8\}\} \end{aligned} \tag{27}$$

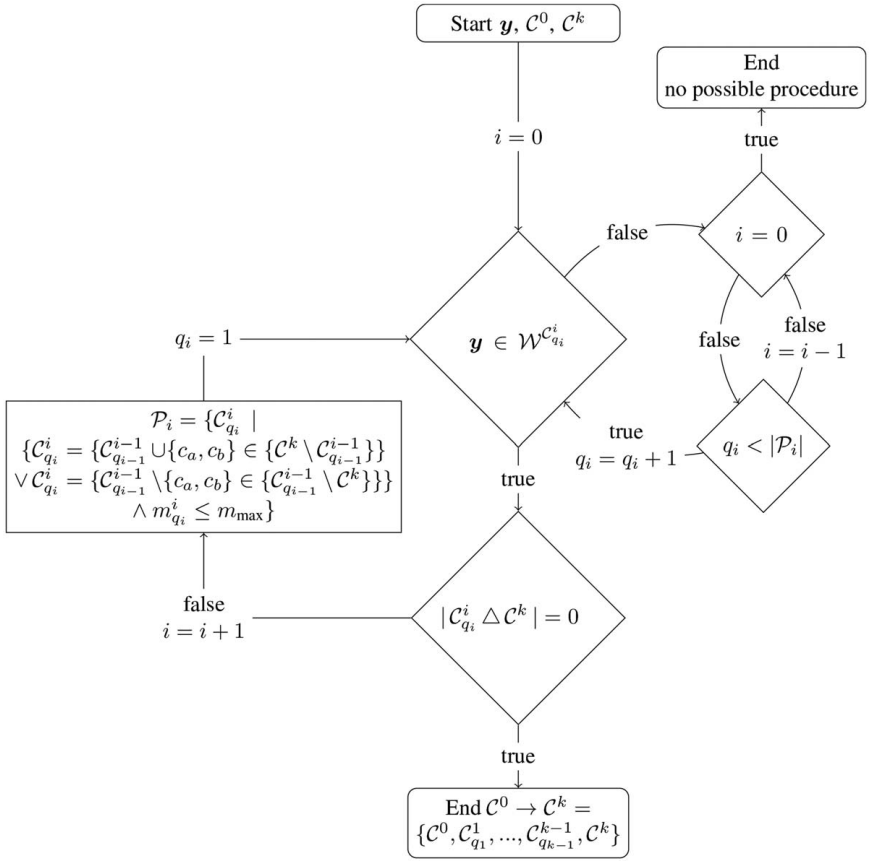

Fig. 3 Algorithm for configuration determination

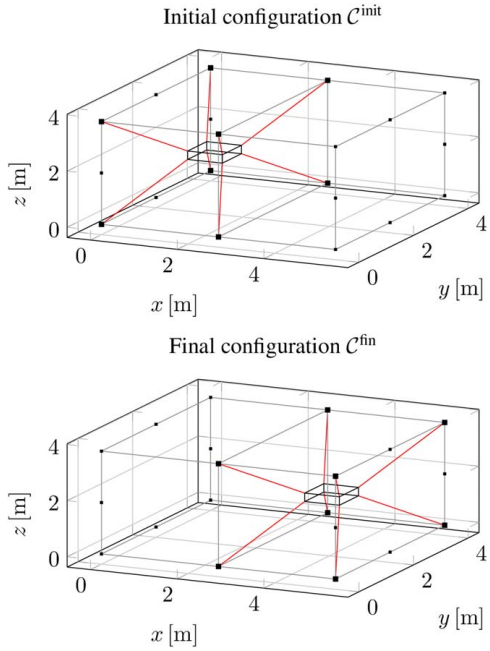

Fig. 4 Initial and final configurations for the simulation experiment

Since the shown CDPRs are completely separate, it is easy to see, that there is no common workspace of the configurations, which requires the use of a transition configuration (examined in Eq. (19)). Although the *COPacabana* offers a total of 16 separate drive trains in these simulations, 12 are considered for the first experiment and 8 for the second. This is due to the fact that by assuming 16 winches, it is possible for all the cables to be part of the transition configuration, which has already been studied by Gagliardini et al. [33].

5.1 Experiment 1: 12 Available Cables. Given the assumption of 12 available cables, it is not possible for both the initial $\mathcal{C}^{\text{init}}$ and the final $\mathcal{C}^{\text{fin}}$ configurations to be part of a transition configuration, as this would require a total of 16 available drive trains. It is therefore necessary to apply the introduced algorithm from Fig. 3 to the defined scenario. Due to the non-overlapping stable workspaces, the first step is to theoretically determine the transition configuration, as shown in Fig. 5(*c*). The distance measure from Eq. (26) leads to the selection of the outermost cables and, due to the identical distances, four randomly selected cables from the middle position. For the transition from $\mathcal{C}^{\text{init}}$ to $\mathcal{C}^{\text{tra}}$ a minimal configuration is determined (see Fig. 5(*b*)), which is formed by four cables from the top and the two lower left cables needed for the transition configuration. The remaining six free cables are then added to the configuration to complete the transition configuration is finally reached. While staying in the transition configuration the CDPR is moved from $\boldsymbol{y}_{\text{init}}$ to $\boldsymbol{y}_{fin}$ and when the pose is reached, the unnecessary cables are removed from the transition configuration, see Fig. 5(*d*). Here, the pose $\boldsymbol{y}_{\text{init}}$ consists of the position $\boldsymbol{r}_{\text{init}} = [1.35, 2, 1.83]$ m and $\boldsymbol{y}_{\text{fin}}$ of $\boldsymbol{r}_{\text{fin}} = [4.05, 2, 1.83]$ m. For both reconfiguration poses $\boldsymbol{y}_{\text{init}}$ and $\boldsymbol{y}_{\text{fin}}$ no platform rotation is taken into account. Finally, the cables required for $\mathcal{C}^{\text{fin}}$ are added until the obsolete cables are removed to arrive at $\mathcal{C}^{\text{fin}}$. The shown pose satisfies the workspace criteria of each intermediate configuration, as it is required by Eq. (25). It can also be seen that the simplifications made between the configurations, i.e., changing only one cable at a time, hold true. The total computation time for the 12 cable scenario is $t = 99.39$ s and for both transitions from $\mathcal{C}^{\text{init}} \rightarrow \mathcal{C}^{\text{tra}}$ and

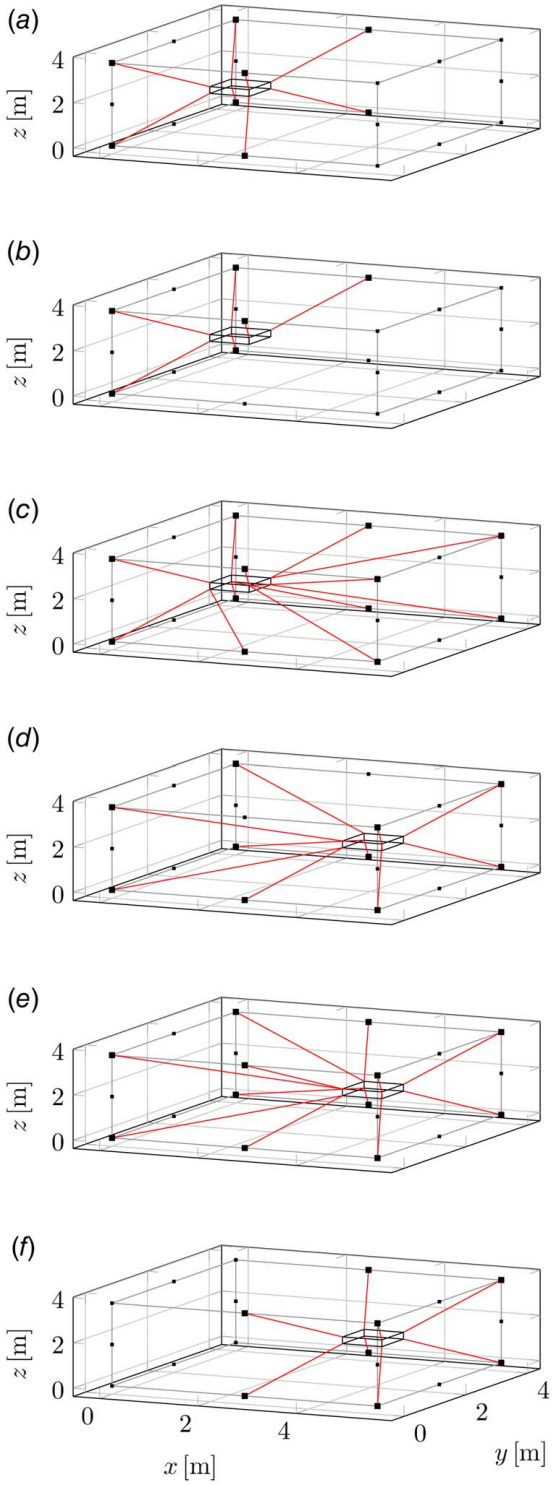

Fig. 5 Resulting reconfiguration sequence for 12 cables starting from $\mathcal{C}^{\text{init}}$ until $\mathcal{C}^{\text{fin}}$: (*a*) initial configuration $\mathcal{C}^{\text{init}}$, (*b*) transition to minimum configuration, (c) transition configuration $\mathcal{C}^{\text{tra}}$, (*d*) pose change $y_{\text{init}} \rightarrow y_{\text{fin}}$ and cable removal $\mathcal{C}^3$, (e) adding the final cables, and (*f*) final configuration $\mathcal{C}^{\text{fin}}$

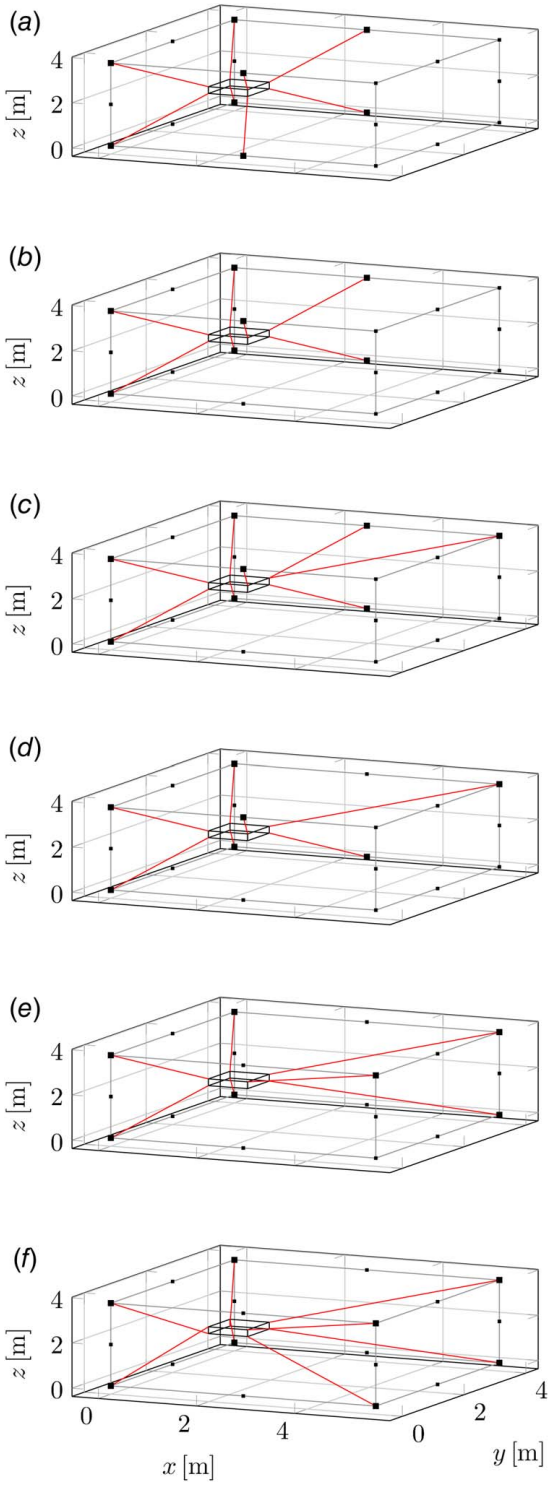

Fig. 6 Resulting reconfiguration sequence for eight cables starting from $\mathcal{C}^{\text{init}}$ until $\mathcal{C}^{\text{fin}}$: (*a*) initial configuration $\mathcal{C}^{\text{init}}$, (*b*) intermediate configuration $\mathcal{C}^1$, (c) intermediate configuration $\mathcal{C}^2$, (*d*) intermediate configuration $\mathcal{C}^3$, (e) intermediate configuration $\mathcal{C}^4$, and (*f*) transition configuration $\mathcal{C}^{\text{tra}}$

$\mathcal{C}^{\text{tra}} \rightarrow \mathcal{C}^{\text{fin}}$ required eight topological reconfigurations. In conclusion, the algorithm works for the 12-cable situation.

5.2 Experiment 2: 8 Available Cables. In the second experiment, the approaches for determining the transition and intermediate configurations are applied to a scenario where the CDPR has eight winches available. This is the more relevant scenario for practical applications, since, the drive trains are the most expensive parts of a CDPR and it is reasonable to have a minimum number of them. As in the experiment from Sec. 5.1, the first step is to define the transition configuration. Again, the

heuristic with theoretical distances is applied and the configuration that spans the largest base area is the result (see Fig. 6(*f*)). The positions for the reconfiguration were also $\boldsymbol{r}_{\text{init}} = [1.35, 2, 1.83]$ m and $\boldsymbol{r}_{\text{fin}} = [4.05, 2, 1.83]$ m. The first step is to remove a cable that is not part of the transition configuration from underneath the platform (see Fig. 6(*b*)). The free cable is then attached to the top of the platform to provide a stabilizing effect, see Fig. 6(*c*). Then, the same procedure is repeated with the other obsolete cable until the transition configuration is reached, see Fig. 6(*f*). The remaining reconfiguration procedure toward the final configuration is not shown here as it is just the symmetric counterpart of the illustrated series of Figs. 6(*a*)–6(*f*). The computation time for the planning algorithm is $t = 102.52$ s and eight reconfigurations were determined from $\mathcal{C}^{\text{init}} \rightarrow \mathcal{C}^{\text{tra}}$ and $\mathcal{C}^{\text{tra}} \rightarrow \mathcal{C}^{\text{fin}}$. The simulated results show that it is possible to reconfigure a CDPR even if there are no additional cables than needed for the redundantly constrained configuration assumed here. However, for practical topological reconfiguration, the availability of 12 or 16 cables has shown to be more advantageous than, e.g., eight cables. The reason for this is that the redundant constraint can be maintained throughout the reconfiguration process, which is beneficial for platform stability. The final section summarizes the results obtained and outlines the next steps.

6 Conclusion and Outlook

In this paper, a strategy for topological in-operation-reconfiguration was introduced. First, reconfigurability was expressed by modeling the CDPR as a general spatial system, without considering usual constant modeling assumptions or kinematic classifications. Second, a stability criterion was introduced and applied to novel definitions of a stable and minimal-stable workspace. Based on these definitions, an algorithm for planning a stable reconfiguration sequence is presented and used in two simulative validation experiments. Both experiments show that it is possible to plan a stable reconfiguration sequence with the presented method. For the future work, there are three main directions that the authors will pursue. First, the theoretical results for the stability assessment will be investigated on the real demonstrator system to check if the stability criterion used works in reality. Second, the computational performance of the algorithms will be optimized to reduce the computation time. One approach will be to introduce additional criteria and constraints into the iterative planning process, to directly exclude configurations and thus shrink the search tree of possible configurations, or to prioritize which configurations should be considered first. Third, a method is developed to automatically detect feasible reconfiguration poses $\boldsymbol{y}$.

Acknowledgment

Supported by the Deutsche Forschungsgemeinschaft (DFG, German Research Foundation) under Germany's Excellence Strategy – EXC 2120/1 – 390831618.

Conflict of Interest

There are no conflicts of interest.

Data Availability Statement

The authors attest that all data for this study are included in the paper.

References

[1] Cone, L. L., 1985, "Skycam, An Aerial Robotic Camera System," Byte Mag., **10**, pp. 122–132.

[2] Kirchgessner, N., Liebisch, F., Yu, K., Pfeifer, J., Friedli, M., Hund, A., and Walter, A., 2016, "The ETH Field Phenotyping Platform FIP: A Cable-Suspended Multi-sensor System," Func. Plant Biol., **44**(1), pp. 154–168.

[3] Miermeister, P., Lachele, M., Boss, R., Masone, C., Schenk, C. T., Tesch, J., Kerger, M., Teufel, H., Pott, A., and Bülthoff, H. H., 2016, "The Cablerobot Simulator Large Scale Motion Platform Based on Cable Robot Technology," 2016 IEEE/RSJ International Conference on Intelligent Robots and Systems (IROS), Daejeon, South Korea, Oct. 9–14, IEEE, pp. 3024–3029.

[4] Pott, A., Mütherich, H., Kraus, W., Schmidt, V., Miermeister, P., and Verl, A., 2012, "IPAnema: A Family of Cable-Driven Parallel Robots for Industrial Applications," *Cable-Driven Parallel Robots* (Vol. 12 of Mechanisms and Machine Science), T. Bruckmann, and A. Pott, eds., Springer, Berlin and Heidelberg, pp. 119–134.

[5] Tempel, P., Hervé, P.-E., Tempier, O., Gouttefarde, M., and Pott, A., 2017, "Estimating Inertial Parameters of Suspended Cable-Driven Parallel Robots: Use Case on CoGiRo," 2017 IEEE International Conference on Robotics and Automation (ICRA), Singapore, May 29–June 3, IEEE, pp. 6093–6098.

[6] Trautwein, F., Reichenbach, T., Tempel, P., Pott, A., and Verl, A., 2020, "COPacabana: A Modular Cable-Driven Parallel Robot," Sechste IFToMM D-A-CH-Konferenz, Lienz, Austria.

[7] Izard, J.-B., Gouttefarde, M., Michelin, M., Tempier, O., and Baradat, C., 2012, "A Reconfigurable Robot for Cable-Driven Parallel Robotic Research and Industrial Scenario Proofing," International Conference on Cable-Driven Parallel Robots (CableCon), Stuttgart, Germany.

[8] Reichert, C., Glogowski, P., and Bruckmann, T., 2015, "Dynamische Rekonfiguration Eines Seilbasierten Manipulators Zur Verbesserung Der Mechanischen Steifigkeit," *Fachtagung Mechatronik 2015: Dortmund (12.03.-13.03.2015)*, T. Bertram, B. Corves, and K. Janschek, eds., Institut für Getriebetechnik und Maschinendynamik, Aachen, Germany, pp. 91–96.

[9] Gagliardini, L., Caro, S., Gouttefarde, M., Wenger, P., and Girin, A., 2015, "A Reconfigurable Cable-Driven Parallel Robot for Sandblasting and Painting of Large Structures," *Cable-Driven Parallel Robots (CableCon 2014)* (Vol. 32 of Mechanisms and Machine Science), A. Pott, and T. Bruckmann, eds., Springer, Cham, pp. 275–291.

[10] Künz GmbH, "Freerider RTG," https://www.kuenz.com/de/cranes/rtg-artg-freerider/.

[11] Nguyen, D. Q., Gouttefarde, M., Company, O., and Pierrot, F., 2014, "On the Analysis of Large-Dimension Reconfigurable Suspended Cable-Driven Parallel Robots," 2014 IEEE International Conference on Robotics and Automation (ICRA), Hong Kong, China, May 31–June 7, IEEE, pp. 5728–5735.

[12] Nguyen, D. Q., and Gouttefarde, M., 2014, "Study of Reconfigurable Suspended Cable-Driven Parallel Robots for Airplane Maintenance," 2014 IEEE/RSJ International Conference on Intelligent Robots and Systems (IROS), Chicago, IL, IEEE, pp. 1682–1689.

[13] Nguyen, D. Q., and Gouttefarde, M., 2014, "Stiffness Matrix of 6-DOF Cable-Driven Parallel Robots and Its Homogenization," *Advances in Robot Kinematics (ARK 2014)*, J. Lenarčič, and O. Khatib, eds., Springer, Cham, pp. 181–191.

[14] Trautwein, F., Reichenbach, T., Pott, A., and Verl, A., 2021, "Workspace Planning for In-Operation-Reconfiguration of Cable-Driven Parallel Robots," *Cable-Driven Parallel Robots* (Vol. 104 of Mechanisms and Machine Science), M. Gouttefarde, T. Bruckmann, and A. Pott, eds., Springer International Publishing, Cham, pp. 182–193.

[15] Zhou, X., Jun, S.-K., and Krovi, V., 2014, "Tension Distribution Shaping Via Reconfigurable Attachment in Planar Mobile Cable Robots," Robotica, **32**(2), pp. 245–256.

[16] Zhou, X., Jun, S.-K., and Krovi, V., 2014, "Stiffness Modulation Exploiting Configuration Redundancy in Mobile Cable Robots," 2014 IEEE International Conference on Robotics ans Automation (ICRA), Hong Kong, China.

[17] Boumann, R., and Bruckmann, T., 2021, "*An Emergency Strategy for Cable Failure in Reconfigurable Cable Robots*," *Cable-Driven Parallel Robots* (Vol. 104 of Mechanisms and Machine Science), M. Gouttefarde, T. Bruckmann, and A. Pott, eds., Springer International Publishing, Cham, pp. 217–229.

[18] Gagliardini, L., Caro, S., Gouttefarde, M., and Girin, A., 2016, "Discrete Reconfiguration Planning for Cable-Driven Parallel Robots," Mech. Mach. Theory, **100**, pp. 313–337.

[19] Gagliardini, L., Gouttefarde, M., and Caro, S., 2018, "*Design of Reconfigurable Cable-Driven Parallel Robots*," *Mechatronics for Cultural Heritage and Civil Engineering* (Vol. 92 of Intelligent Systems, Control and Automation: Science and Engineering), E. Ottaviano, A. Pelliccio, and V. Gattulli, eds., Springer International Publishing, Cham, pp. 85–113.

[20] Mishra, U. A., Caro, S., and Gouttefarde, M., 2021, "Optimizing Cable-Routing for Reconfigurable Cable-Driven Parallel Robots," 5th IEEE/IFToMM International Conference on Reconfigurable Mechanisms and Robots (ReMAR), Toronto, Canada.

[21] Gagliardini, L., 2016, "Discrete Reconfigurations of Cable-Driven Parallel Robots," Ph.D. thesis, Université Nantes-Angers-Le Mans, Nantes, France.

[22] Behzadipour, S., and Khajepour, A., 2006, "Stiffness of Cable-Based Parallel Manipulators With Application to Stability Analysis," ASME J. Mech. Des., **128**(1), pp. 303–310.

[23] Behzadipour, S., and Sohi, M. A., 2007, "Antagonistic Stiffness in Cable-Driven Mechanisms," 12th IFToMM World Congress on Mechanism and Machine Science 2007, Besancon, France.

[24] Carricato, M., and Merlet, J.-P., 2013, "Stability Analysis of Underconstrained Cable-Driven Parallel Robots," IEEE Trans. Rob., **29**(1), pp. 289–296.

[25] Pott, A., and Tempel, P., 2019, "*A Unified Approach to Forward Kinematics for Cable-Driven Parallel Robots Based on Energy*," *Advances in Robot Kinematics (ARK 2018)* (Vol. 8 of Springer Proceedings in Advanced Robotics), J. Lenarčič, and V. Parenti-Castelli, eds., Springer, Cham, pp. 401–409.
[26] Gosselin, C. M., and Angeles, J., 1990, "Singularity Analysis of Closed-Loop Kinematic Chains," IEEE Trans. Rob. Autom., **4**(3), pp. 281–290.
[27] Pott, A., 2018, *Cable-Driven Parallel Robots: Theory and Application*, Vol. 120, Bruno Siciliano, Oussama Khatib, eds., Springer, Cham.
[28] Ming, A., and Higuchi, T., 1994, "Study on Multiple Degree-of-Freedom Positioning Mechanism Using Wires (Part 1): Concept, Design and Control," Int. J. Jpn. Soc. Precis. Eng., **28**(2), pp. 131–138.
[29] Ming, A., and Higuchi, T., 1994, "Study on Multiple Degree-of-Freedom Positioning Mechanism Using Wires (Part 2): Development of a Planar Completely Restrained Positioning Mechanism," Int. J. Jpn. Soc. Precis. Eng., **28**(3), pp. 235–242.
[30] Kraus, W., Schmidt, V., Pott, A., and Verl, A., 2012, "Investigation on a Planar Cable-Driven Parallel Robot," Proceedings of the 7th German Conference Robotics (ROBOTIK 2012), VDE-Verlag, Frankfurt am Main, pp. 193–198.
[31] Pott, A., Bruckmann, T., and Mikelsons, L., 2009, "*Closed-Form Force Distribution for Parallel Wire Robots*," *Computational Kinematics*, A. Kecskeméthy, and A. Müller, eds., Springer, Berlin and Heidelberg, pp. 25–34.
[32] Pott, A., 2018, "*Efficient Computation of the Workspace Boundary, Its Properties and Derivatives for Cable-Driven Parallel Robots*," *Computational Kinematics* (Vol. 50 of Mechanisms and Machine Science), S. Zeghloul, L. Romdhane, and M. A. Laribi, eds., Springer International Publishing, Cham, pp. 190–197.
[33] Gagliardini, L., Gouttefarde, M., and Caro, S., 2016, "Determination of a Dynamic Feasible Workspace for Cable-Driven Parallel Robots," 15th International Conference on Advances in Robot Kinematics 2016, Grasse, France, Springer, pp. 365–374.